

The Temporal Evolution of Thermal Instability in Fluid Layers Isothermally Heated from Below

Tae Joon Chung, Min Chan Kim* and Chang Kyun Choi†

School of Chemical Engineering, Seoul National University, Seoul 151-744, Korea

*Department of Chemical Engineering, Cheju National University, Cheju 690-756, Korea

(Received 16 March 2003 • accepted 15 July 2003)

Abstract—The temporal development of thermal disturbances in the fluid layer heated isothermally from below is investigated, based on propagation theory. This theory is examined by using scaling. To examine the behavior of thermal instability the mean-field approximation is employed and resulting equations are solved by Galerkin method. The stability criteria to mark the onset of convective instability are newly suggested as the intersection point of the growth rate of averaged temperature with that of its fluctuation. The resulting critical time is close to that derived from propagation theory. By considering the nonlinear effects, the characteristic times to represent the detection time of manifest convection and also to exhibit the minimum Nusselt number are discussed.

Key words: Mean-field Approximation, Natural Convection, Propagation Theory

INTRODUCTION

When a fluid layer is heated from below, it becomes potentially unstable by the buoyancy forces due to the inverse density gradient. This phenomenon is familiar to anyone who has observed the shimmering of air. The mechanism of such convective flow is responsible for some great ocean currents and for the global circulation of the atmosphere. Since systematic experiments of Bénard [1901] and linear stability theory of Lord Rayleigh [1916] were introduced, a great deal of work has been conducted in the field of mathematics, physics and engineering. Buoyancy-driven convection plays an important role in conventional heat and mass transfer systems, materials processing requiring uniformity of products, and in the design of reactors. In many practical processes, a sudden heating or cooling with a high temperature gradient is more common. Buoyancy-driven convection can occur before the temperature profile in the basic state becomes fully developed. Therefore, it is important to know when or where the buoyancy-driven convection sets in.

For a system having a time-dependent nonlinear temperature profile, the onset of natural convection was first investigated theoretically by Morton [1957] and experimentally by Soberman [1959], respectively. Foster [1965] developed the amplification theory, which uses an initial value technique to match disturbances with time in the system. This theory requires the amplification factor to represent the detection time of manifest convection. With the mean-field approximation involving nonlinear convective terms Herring [1963, 1964] analyzed the fully developed heat transport. Elder [1969] examined the time-dependent development of convective motion with the mean-field approximation by using the finite difference scheme. Using a stochastic model, Jhaveri and Homsy [1982] defined the onset of convective motion by comparing the convective heat transport with the conductive one. They employed stochastic white noise

as an initial condition. Hohenberg and Swift [1992] suggested a model where the Langevin noise term inducing convective motion is used as an initial condition.

Recently, the onset of natural convection has been analyzed in various time-dependent systems by using propagation theory [Choi et al., 1998; Kang et al., 2000; Kim et al., 2002; Yang and Choi, 2002]. However, there exists some difference between the predicted onset times derived from propagation theory and available experimental data. In the present study the propagation theory is re-examined by using scaling and with the stability criteria from the propagation theory the Oberbeek-Boussinesq equations are solved by the Galerkin method. The new stability criteria are suggested by comparing the temporal growth rate of the conduction temperature field with that of fluctuations. The present study is concerned with the case of a large Prandtl number Pr , especially $Pr \rightarrow \infty$, and the characteristic time to mark the detection of manifest convection is discussed in comparison with available theoretical predictions and experimental data.

GOVERNING EQUATIONS

The system considered here is an initially quiescent Newtonian fluid between the two horizontal rigid plates heated from below, as shown in Fig. 1. Here Z denotes the vertical distance. The temper-

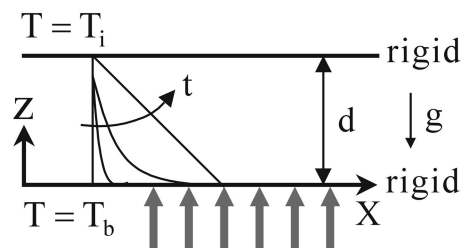


Fig. 1. Schematic diagram of conduction state considered in the present study.

†To whom correspondence should be addressed.

E-mail: ckchoi@snu.ac.kr

ature of fluid is T_i for time $t \leq 0$ and for $t > 0$ there is a step change in the bottom temperature to a higher value T_b . For a large $\Delta T (= T_b - T_i)$, thermal instabilities inducing buoyancy forces will set in at a certain time and grow with time. Based on the Boussinesq approximation, the proper dimensionless governing equations are represented by

$$\left(\frac{1}{\text{Pr}} \frac{\partial}{\partial \tau} - \nabla^2 \right) \nabla^2 \mathbf{u} = \frac{1}{\text{Pr}} \nabla \times (\nabla \times (\mathbf{u} \cdot \nabla \mathbf{u})) + \text{Ra} \nabla \times (\nabla \times \mathbf{e}_k \theta), \quad (1)$$

$$\left(\frac{\partial}{\partial \tau} + \mathbf{u} \cdot \nabla \right) \theta = \nabla^2 \theta, \quad (2)$$

where \mathbf{u} , θ , τ and \mathbf{e}_k denote the velocity vector, the temperature, the time, and the unit vector in the z -direction, respectively. Here d , d^2/α , α/d and ΔT are scaling factors for distance, time, velocity, and temperature, respectively. Symbols d and α denote the fluid depth and the thermal diffusivity, respectively. Eq. (1) has been obtained by eliminating the pressure from equations of continuity and motion. The important dimensionless parameters, the Prandtl number Pr and the Rayleigh number Ra , are defined as

$$\text{Pr} = \frac{\nu}{\alpha} \quad \text{and} \quad \text{Ra} = \frac{g\beta\Delta T d^3}{\alpha\nu}, \quad (3a-b)$$

where ν , α and β are the kinematic viscosity, the gravitational acceleration and the thermal expansion coefficient, respectively.

PROPAGATION THEORY

By following the well-known linear stability analysis the infinitesimal perturbation quantities \mathbf{u}_1 and θ_1 are superimposed on the basic quantities \mathbf{u}_0 and θ_0 , respectively. Since the present system is initially quiescent, $\mathbf{u}_0 = \mathbf{0}$. For the regular convective motion, the dimensionless vertical velocity component w_1 and the temperature one θ_1 can be described as

$$(w_1, \theta_1) = (w_*, \theta_*) \exp[i(a_x x + a_y y)], \quad (4)$$

where the subscript $*$ and i denote the perturbed amplitude function and the imaginary number, respectively. Here a_x and a_y represent the dimensionless wavenumbers along the x - and y -direction, respectively. Based on the above normal mode of disturbances, the propagation theory assumes that the thermal disturbances at the critical onset time to mark the onset of a fastest growing instability are propagated mainly within the thermal boundary layer [Yang and Choi, 2002].

Under this assumption the scaling balances between viscous and buoyancy forces in the Z -component of the equation of motion

$$\frac{w_1}{\Delta_r^2} \sim g\beta T_1, \quad (5)$$

where Δ_r is the thermal boundary-layer thickness. From the above relation the scaling relationship of $w_1/(Ra\theta_1) \sim \delta_r^2 \sim \tau$ can be derived. Here $\delta_r (= \Delta_r/d)$ is the dimensionless thermal boundary-layer thickness with $\delta_r \propto \tau^{1/2}$. For a given Ra , the velocity and temperature disturbances are assumed to have the form of $w_* = \tau^{n+1} w^*(\zeta)$ and $\theta_* = \tau^n \theta^*(\zeta)$, where $\zeta (= z/\sqrt{\tau})$ represents the similarity variable. Now, the new stability equations are produced self-similarly from Eqs. (1) and (2):

$$\left\{ (D^2 - a^{*2})^2 + \frac{1}{2\text{Pr}} [\zeta D^3 - a^{*2} \zeta D + (2n+2)a^{*2}] \right\} w^* = \text{Ra}^* a^{*2} \theta^*, \quad (6)$$

$$\left(D^2 + \frac{1}{2} \zeta D - a^{*2} - n \right) \theta^* = w^* D \theta_0, \quad (7)$$

with the following boundary conditions

$$w^* = D w^* = \theta^* = 0 \quad \text{at} \quad \zeta = 0 \quad \text{and} \quad \zeta = 1/\sqrt{\tau}, \quad (8)$$

where $D = d(\cdot)/d\zeta$, $\text{Ra}^* = \text{Ra} \tau^{2/2}$ and $a^* = a \tau^{1/2}$ with $a = \sqrt{a_x^2 + a_y^2}$. Here τ is regarded as parameter, i.e., $\tau = \tau_c$ at critical condition.

For deep-pool systems, the upper boundary of $\zeta = 1/\sqrt{\tau}$ approaches the infinite as $\tau \rightarrow 0$. The basic temperature, θ_0 , which is the temperature profile in conduction state, is described by

$$\theta_0 = 1 - \text{erf}\left(\frac{\zeta}{2}\right) \quad \text{as} \quad \tau \rightarrow 0. \quad (9)$$

For given Pr and a^* the minimum value of Ra^* is calculated numerically. Then the minimum value of τ , i.e., τ_c^* , and its corresponding wavenumber a_c is obtained for given Pr and Ra . The minimum value of Ra^* increases with increasing $n (\geq 0)$ and the case of $n=0$ constitutes the minimum bound, as shown in Fig. 2. If $n < 0$, it is irrational since $\theta_c \rightarrow \infty$ as $\tau \rightarrow 0$ near $z=0$. This procedure can be extended to the whole time domain by fixing τ in Eqs. (6)-(8) [Yang and Choi, 2002; Kim et al., 2002]. For $\tau \rightarrow \infty$ we can obtain the well-known critical values, $\tau = 1,708$ and $a_c = 3.12$, which correspond to the case of the fully developed, linear temperature profile.

From marginal stability curves shown in Fig. 2, the stability criteria to mark the onset of thermal instability are obtained:

$$\tau_c^* = 7.54 \text{Ra}^{-2/3} \quad \text{with} \quad a_c = 0.197 \text{Ra}^{1/3} \quad \text{as} \quad \tau \rightarrow 0 \quad \text{and} \quad \text{Pr} \rightarrow \infty \quad (10)$$

At the condition of $\tau_c^* = 1.6 \times 10^{-2}$ with $\text{Ra} = 10^4$ the normalized amplitudes of velocity and temperature disturbances are shown in Fig. 3. For $\text{Pr} \rightarrow \infty$, the velocity amplitude w_* covers the whole domain while the temperature one, θ_* exists mainly within δ_r . It seems evi-

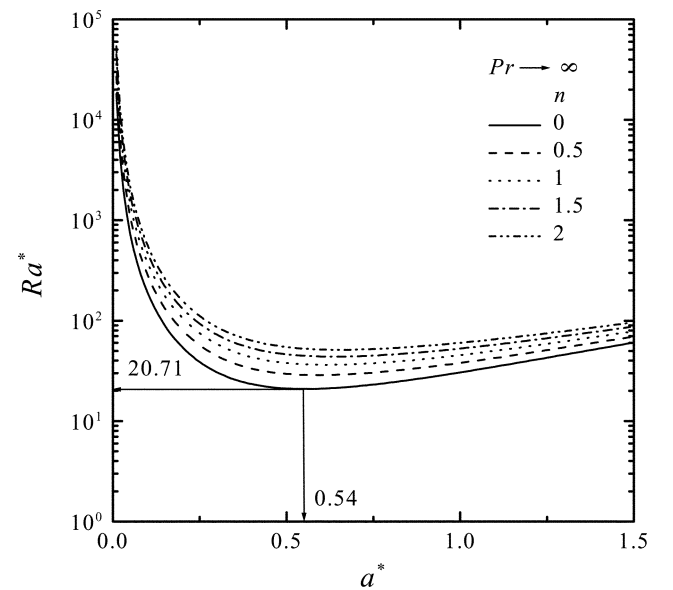


Fig. 2. Marginal stability curves for $\tau \rightarrow 0$. The minimum of Ra^* value = 20.71 with $a_c^* = 0.54$ for $n \geq 0$.

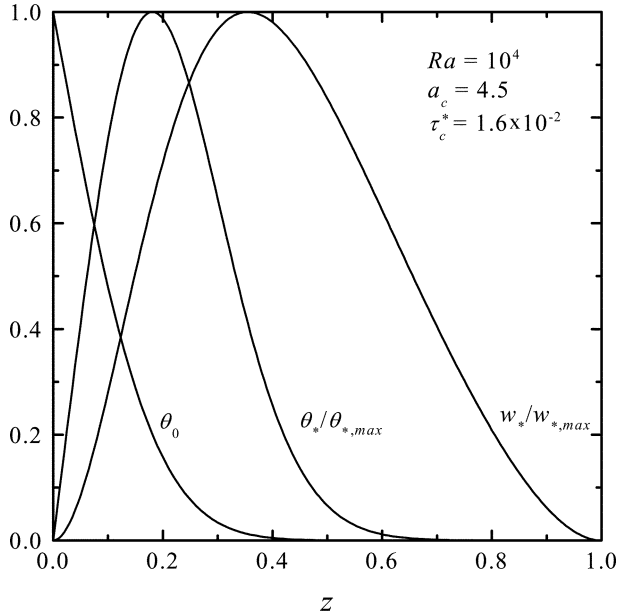


Fig. 3. Amplitude profiles of basic temperature and normalized temperature and velocity disturbances.

dent that the thermal disturbances are propagated mainly within the thermal boundary layer until the temperature profiles deviate from the conduction state and then disturbances are amplified enough to be detected with naked eyes or thermocouples. The validity of this statement is challenged below by using the Galerkin method.

GROWTH OF DISTURBANCES

1. Mean-Field Approximation

In the present study we employ the mean-field approximation suggested by Herring [1964]. For initially quiescent fluid layer the temperature and velocity fields are divided into the sum of a horizontal mean and its fluctuating part:

$$\theta(\tau, x, y, z) = \langle \theta(\tau, z) \rangle + \theta'(\tau, x, y, z), \quad (11a)$$

$$w(\tau, x, y, z) = \langle w(\tau, z) \rangle + w'(\tau, x, y, z). \quad (11b)$$

Here $\langle \cdot \rangle$ denotes the horizontally averaged one and the superscript ' represents the deviation from the mean temperature. The resulting mean-field equations are obtained by introducing Eqs. (11) into (1) and (2):

$$\left(\frac{1}{\text{Pr}} \frac{\partial}{\partial \tau} - \nabla^2 \right) \nabla^2 w' = \text{Ra} \nabla_i^2 \theta' + \frac{M}{\text{Pr}}, \quad (12)$$

$$\left(\frac{\partial}{\partial \tau} - \nabla^2 \right) \theta' = -w' \frac{\partial \langle \theta \rangle}{\partial z} + H, \quad (13)$$

$$\left(\frac{\partial}{\partial \tau} - \frac{\partial}{\partial z^2} \right) \langle \theta \rangle = -\frac{\partial}{\partial z} \langle w' \theta' \rangle, \quad (14)$$

where $\nabla_i^2 = \partial^2/\partial x^2 + \partial^2/\partial y^2$. The terms H and M represent the fluctuating self-interactions owing to advection of heat and momentum, i.e., $\mathbf{u} \cdot \nabla(\cdot)$. For $\text{Pr} \rightarrow \infty$ the nonlinear term M in Eq. (12) can be negligible. Since the mean temperature gradients are large near the bottom boundary, H can be negligible in the bulk of the flow. These are well illustrated by the work of Herring [1963] and Elder

[1969]. The proper boundary conditions are

$$w' = \partial w'/\partial z = \theta' = \langle \theta \rangle - 1 = 0 \quad \text{at } z=0, \quad (15a)$$

$$w' = \partial w'/\partial z = \theta' = \langle \theta \rangle = 0 \quad \text{at } z=1. \quad (15b)$$

2. Galerkin Method

When ignoring the convective terms of fluctuations, the well-known linear stability equations are recovered from Eqs. (12)-(15). In order to treat the transient behavior of thermal instabilities, the Galerkin method is employed. The two-dimensional velocity and temperature disturbances are assumed by a series of specified spatial functions with time-dependent amplitude coefficients like Eq. (4):

$$w'(\tau, x, z) = w_* \cos(ax), \quad (16)$$

$$\theta'(\tau, x, z) = \theta_s \cos(ax), \quad (17)$$

$$\langle \theta(\tau, z) \rangle = 1 - z + 2 \sum_{n=1}^{\infty} \frac{C_n(\tau)}{n\pi} \sin(n\pi z), \quad (18)$$

where $w_* = \sum_{n=1}^{\infty} A_n(\tau) \sin(n\pi z) \sin(n\pi z)$ and $\theta_s = \sum_{n=1}^{\infty} B_n(\tau) \sin(n\pi z)$. These

functions automatically satisfy the boundary conditions. The trial functions of w_* and θ_s are the same as those of Gresho and Sani [1971]. By substituting Eqs. (16)-(18) into (12)-(14) and using the orthogonality of the trial functions we obtain the following linear set of $3N$ simultaneous, first-order differential equations for the amplitude coefficients:

$$\frac{dA_k}{d\tau} = -\text{Pr}[(k^2+1)\pi^2 + a^2]A_k + \frac{4a^2 \text{PrRa}}{[(k^2+1)\pi^2 + a^2]} \sum_{m=1}^N B_m \mathbf{H}_{km}, \quad (19)$$

$$\frac{dB_k}{d\tau} = -[k^2\pi^2 + a^2]B_k + 2 \left[\sum_{m=1}^N A_m \mathbf{H}_{km} - 2 \sum_{m=1}^N \sum_{n=1}^N A_m C_n \mathbf{K}_{kmn} \right], \quad (20)$$

$$\frac{dC_k}{d\tau} = -k^2\pi^2 C_k - \frac{k\pi}{2} \left[\sum_{j=1}^N \sum_{m=1}^N A_j B_m \mathbf{N}_{klm} \right], \quad (21)$$

where $k=1, 2, 3, \dots, N$. The matrices \mathbf{H}_{km} , \mathbf{K}_{kmn} and \mathbf{N}_{klm} have the following elements:

$$\mathbf{H}_{km} = \int_0^1 \sin(k\pi z) \sin(\pi z) \sin(m\pi z) dz, \quad (22a)$$

$$\mathbf{K}_{kmn} = \int_0^1 \sin(k\pi z) \sin(\pi z) \sin(m\pi z) \cos(n\pi z) dz, \quad (22b)$$

$$\mathbf{N}_{klm} = \int_0^1 \frac{d}{dz} \{ \sin(m\pi z) \sin(\pi z) \sin(l\pi z) \} \sin(k\pi z) dz. \quad (22c)$$

The above amplitude Eqs. (19)-(21) need the rational initial conditions but they cannot be specified at $\tau=0$. Therefore the calculation starts at $\tau = \tau_c \ll \tau_c^*$. At $\tau = \tau_c$, the normalized quantities of disturbance amplitudes derived from the propagation theory are given with proper magnitudes of w_* and θ_s in Eqs. (16) and (17), i.e., w_{*i} and θ_{*i} , and mean temperature is obtained from Eq. (18). In the present study we set $\tau_c = 10^{-4}$. Then the initial coefficients are expressed as

$$A_k(\tau_i) = 2 \int_0^1 w_{*i} w_p(\tau_c^*, z) \sin(\pi z) \sin(k\pi z) dz, \quad (23)$$

$$B_k(\tau_i) = 2 \int_0^1 \theta_{*i} \theta_p(\tau_c^*, z) \sin(k\pi z) dz, \quad (24)$$

$$C_k(\tau_i) = \exp(-k^2\pi^2 \tau_i), \quad (25)$$

$$Nu = \frac{q_w d}{k \Delta T} = 1 - 2 \sum_{k=1}^N C_k(\tau), \quad (26)$$

where w_p and θ_p are the normalized profiles at $\tau = \tau_c^*$ (see Fig. 3) and Nu , q_w , and k denote the Nusselt number, the heat flux at the bottom wall, and the thermal conductivity, respectively. Now, Eqs. (19)-(21) can be integrated from $\tau = 10^{-4}$ until the desired time. The integration is done numerically by using Gear's BDF method which can treat the stiffness of nonlinear terms. If the coupled convective term $\langle w'\theta' \rangle$ does not exist in Eq. (14), less than 20 Fourier coefficients are enough to describe development of fluctuations, as was done by Foster [1965]. We chose $\Delta\tau = 10^{-4}$ with 120 Fourier terms. The calculated values A_k , B_k and C_k are compared with the predicted ones of the previous time within the error tolerance of $O(10^{-6})$.

Since we treat the case of $Pr \rightarrow \infty$, it is clear that $dA_k/d\tau = 0$ in Eq. (19). By choosing the proper θ_{τ} -value we can proceed with the present Galerkin scheme, starting from $\tau = \tau_c$.

RESULTS AND DISCUSSION

1. Fully Developed State

In the fully developed region with $Ra = 10^4$ and $Pr \rightarrow \infty$, the profiles of the mean-field temperature and fluctuations are shown in Fig. 4. Here a_c for a fastest growing mode has been obtained from the propagation theory. It is known that the quantities except w' are seriously distorted from the initial shapes given in Fig. 3. Such a behavior stresses the nonlinear coupling effect caused by the term $\langle w'\theta' \rangle$ in the present system. The profiles of θ' and $\langle \theta \rangle$ show that the conduction layers exist near the upper and lower boundaries.

Table 1 shows that for $Ra = 10^4$ and $a = 9$ there is a small difference in Nu according to the choice of numerical technique. In the present study we used the 120 Fourier coefficients and the trial functions defined by Gresho and Sani [1971] while Herring [1964] used the Green function based on multiple wavenumbers and Elder [1969] employed the finite difference method. The present results show

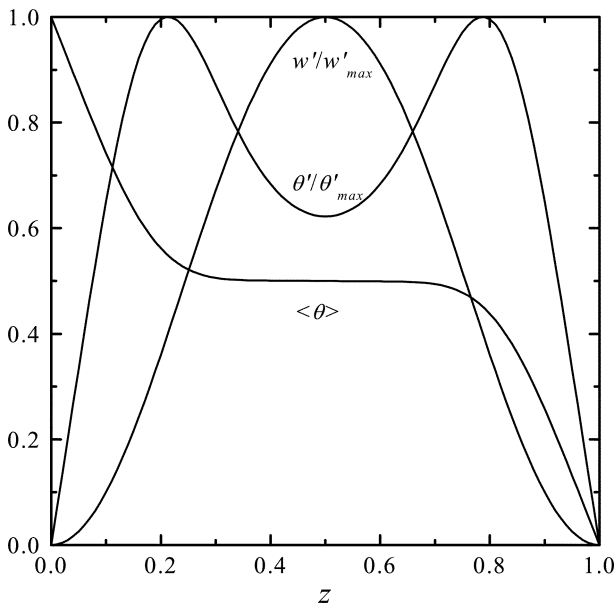


Fig. 4. Fully developed profiles of basic and fluctuation quantities for $Ra = 10^4$ and $a_c = 4.5$.

Table 1. Comparison of present results with available ones in fully developed state of $Ra = 10^4$ and $a = 9$

| | w'_{max} | θ'_{max} | Nu |
|----------------|------------|-----------------|-------|
| Present study | 29.77 | 0.1847 | 2.788 |
| Herring [1964] | 21.95 | 0.185 | 2.824 |
| Elder [1969] | 21.912 | 0.1847 | 2.823 |

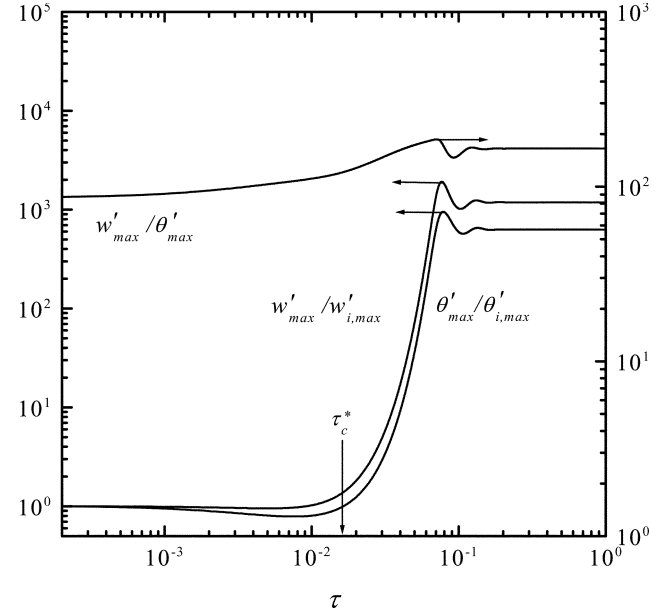


Fig. 5. Temporal evolution of disturbances for $Ra = 10^4$ and $a_c = 4.5$.

that the present Galerkin method is valid at $Ra = 10^4$.

2. Temporal Evolution of Disturbances at $Ra = 10^4$

The temporal evolution of the fluctuation fields for $Ra = 10^4$ is shown in Fig. 5. Here the maximum values of w' and θ' have been normalized by their initial maximum magnitudes $w'_{i,max}$ and $\theta'_{i,max}$. Up to $\tau = \tau_c^*$ there is no significant change in the amplitudes of fluctuation quantities. As Mahler et al. [1968] commented that the initial disturbances would be constant, such a behavior is shown in this time domain of $0 \leq \tau \leq \tau_c^*$. The ratio of w'_{max} to θ'_{max} increases slowly up to $\tau = \tau_c^*$. For $\tau > \tau_c^*$, there is a super exponential growth of disturbances since the temperature field has been developed to an appreciable extent. In the fully developed region the fluctuation amplitude behaves like a damped oscillator and eventually converges to a constant value due to the effect of the nonlinear term, i.e., $\langle w'\theta' \rangle$.

Fig. 6 shows that for $0 < \tau < \tau_u$ the heat transport seems to be governed by conduction. Here τ_u is called the undershoot time. Manifest convection exists for $\tau \geq \tau_u$. For small time the heat transfer rate under the conduction state decreases with $t^{1/2}$ while the thermal boundary-layer thickness increases with $t^{1/2}$. However, after manifest convection is detected, the heat transfer rate starts to increase with time and the Nusselt number Nu starts to deviate from that of conduction. Jhaveri and Homay [1982] regarded the detection time of manifest convection as that time when the Nu -value is 1% larger than that of conduction state. With $\theta_{\tau} = 10^{-3}$, the predicted τ_u -value is close to that in available experiments [Patrick and Wragg, 1975; Inoue et al., 1983]. Therefore it may be stated that $\tau_u \cong 4\tau_c^*$ in the actual system.

Here we employ the root-mean-square (rms) quantity in order to

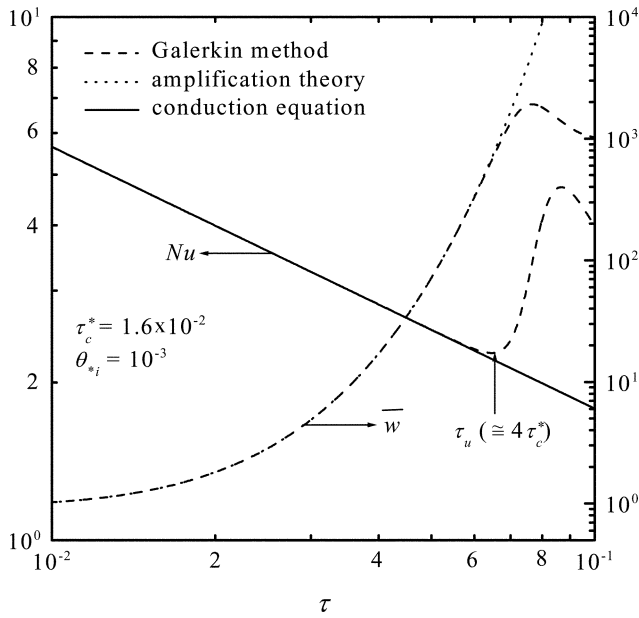


Fig. 6. Nusselt number Nu and amplification factor \bar{w} as a function of time τ for $Ra=10^4$ and $a_c=4.5$.

examine the quantitative behavior of temporal growth of disturbances:

$$(\cdot)_{rms} = \left[\frac{1}{V} \int_V (\cdot)^2 dV \right]^{1/2} \quad (27)$$

where V is the total volume of the system considered. The rms concept is applied to both the velocity and the temperature fields. Foster [1965] proposed the so-called amplification factor using the rms value of vertical velocity normalized with the initial value, i.e., $\bar{w}(\tau) = w_{e,rms}(\tau)/w_{e,rms}(\tau_i)$. From the linearized equations of (12)-(14) the amplification theory is recovered. But this theory loses its validity when the effect of nonlinear term $\langle w'\theta' \rangle$ becomes significant. Gresho and Sani [1971] assumed that $\bar{w} = 10^3$ at the detection time of manifest convection. For $Ra=10^4$, our results show that $\tau_c^* = 1.6 \times 10^{-2}$ with $a_c=4.5$ and $\bar{w} = 697$ at $\tau = \tau_u$, as shown in Fig. 6. In the figure it is shown that linear theory is valid until $\tau \approx \tau_u$. The coupled nonlinear term plays a significant role for $\tau > \tau_u$.

To clarify the detection time of manifest convection we introduce the following growth rates using the rms values of mean temperature and its fluctuations:

$$r_0 = \frac{1}{\langle \theta \rangle_{rms}} \frac{d\langle \theta \rangle_{rms}}{d\tau}, \quad r_1 = \frac{1}{\theta'_{rms}} \frac{d\theta'_{rms}}{d\tau}, \quad (28a-b)$$

where r_0 and r_1 represent the growth rates of mean temperature and its fluctuations, respectively. For small time $r_0 = 1/(4\tau)$ from Eq. (9). Their temporal behavior is shown in Fig. 7. For $\tau < \tau_c$, r_0 is larger than r_1 . The fluctuations are deamplified for $r_1 < 0$ and τ_c^* exists near τ_c . The r_1 -value reaches the maximum $r_{1,max}$ at $\tau = \tau_{r1,max}$ and then it decreases sharply with time. Considering $\tau_u \approx \tau_{r1,max}$, it is supposed that manifest convection would be detected near these characteristic times. The critical time τ_c may be called the onset time of intrinsic instability because τ_c is independent of magnitude of θ_{si} with $\tau_c < \tau_c^*$. As shown in the figure, however, $\tau_{r1,max}$ is sensitive to the magnitude of θ_{si} .

3. Large-Ra Case

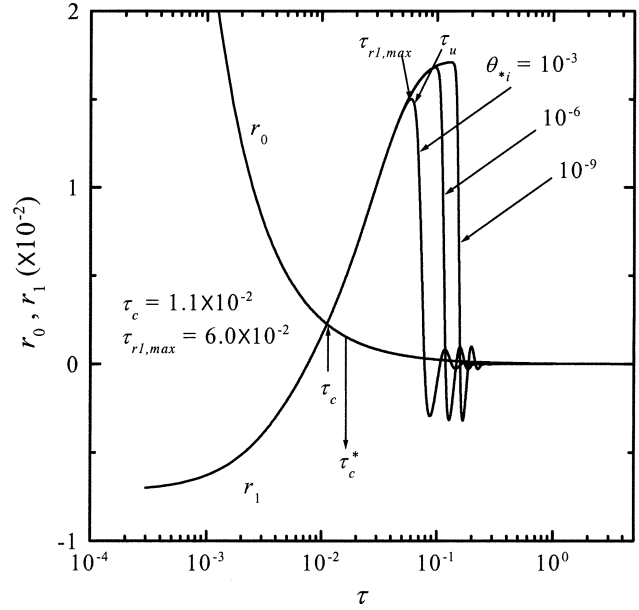


Fig. 7. Comparison of growth rate of mean temperature with its perturbed one for $\theta_{si}=10^{-3}, 10^{-6}, 10^{-9}$ with $Ra=10^4$ and $a_c=4.5$.

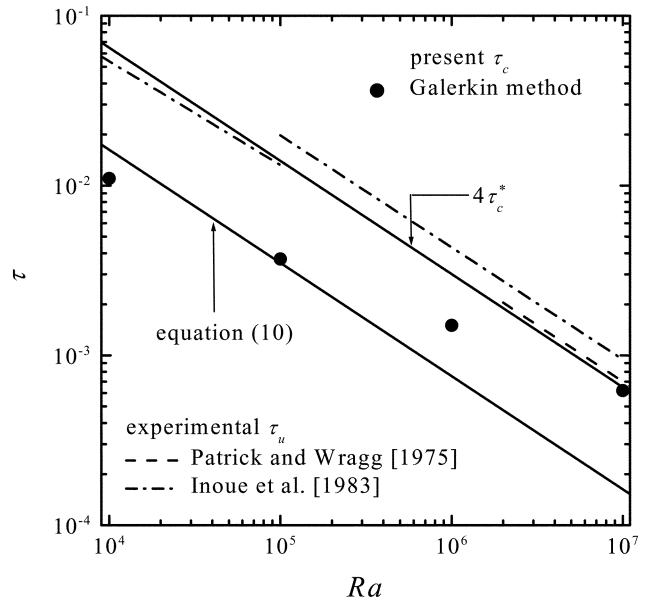


Fig. 8. Comparison of characteristic times with experimental data.

For $Ra=10^5, 10^6$ and 10^7 , the above Galerkin scheme with $\theta_{si}=10^{-3}$ has been used in obtaining τ_c, a_c, r_1 and Nu . Here a_c is chosen as the critical value like that of $Ra=10^4$, with which the earliest time τ_c to reach $r_1=r_0$ is obtained. In Fig. 8, τ_c is compared with τ_c^* . For $Pr > 2000$ the experimental τ_u -values of Patrick and Wragg [1975] and Inoue et al. [1983] are located near $\tau \approx 4\tau_c^*$.

Fig. 9 shows the critical wavenumbers obtained from several models. For large Ra , the a_c -values from the Galerkin method are much smaller than the others. For $Ra=10^5$, the present Galerkin scheme yields $\tau_c = 3.7 \times 10^{-3}$ with $a_c=5.5$ while the propagation theory does $\tau_c^* = 3.5 \times 10^{-3}$ with $a_c=9.1$ from Eq. (10). The onset of convective

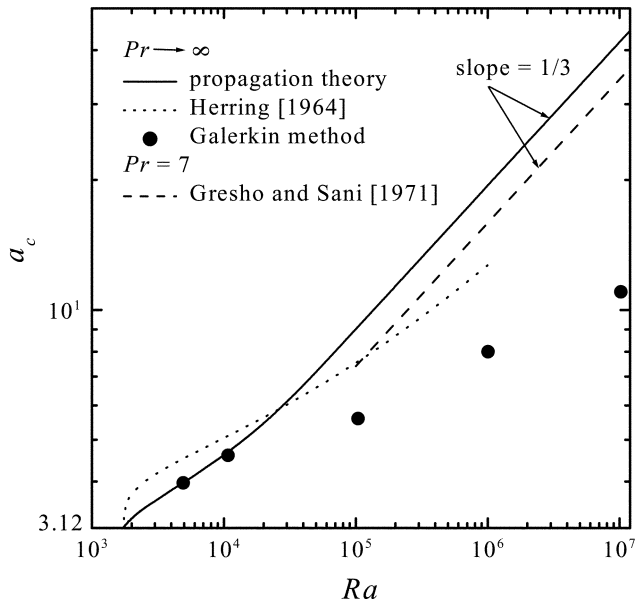


Fig. 9. Comparison of critical wave numbers from various models.

motion is first detected experimentally at $\tau = \tau_m$, which is usually a little smaller than τ_u . It is supposed that with the proper θ_s -value, e.g. $\theta_s = 10^{-3}$, $\tau_m = \tau_{r_1, max}$. From the amplification theory, Gresho and Sani [1971] obtained $\tau_m = 1.4 \times 10^{-2}$ with $a_c = 6.75$ while Foster [1968] did $\tau_m = 1.2 \times 10^{-2}$ with $a_c = 5.8$. These predictions show that $\tau_c \cong \tau_c^*$ and $\tau_m \cong \tau_u \cong 4\tau_c^*$, and the a_c -value from the Galerkin method is close to Foster's. The Nu-values obtained from the Galerkin method agree well with the experimental data of Koschmieder and Pallas [1974] for $Ra \leq 10^5$. But it is concluded that the present Galerkin scheme is useful for $Ra \leq 10^4$ because $\tau_c^* > \tau_c$ at $Ra = 10^5$.

Elder [1969] analyzed the system, based on the growth rate of the spatial maximum value of temperature fluctuations at each instant.

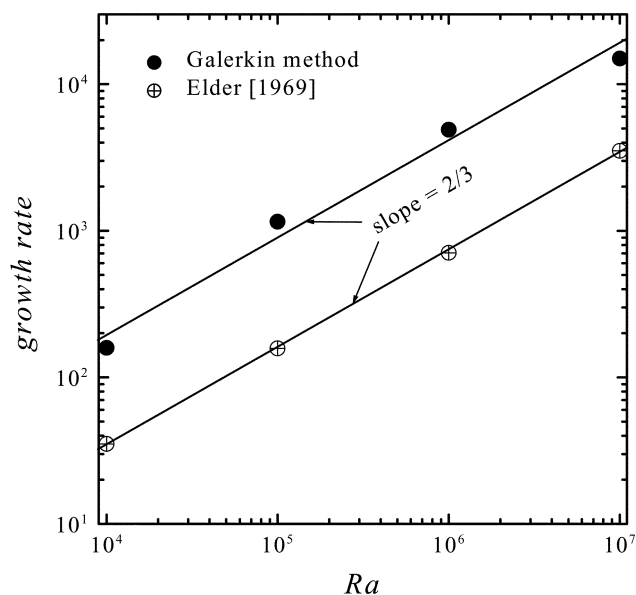


Fig. 10. Comparison of the present growth rate $r_{1, max}$ with Elder's.

The present $r_{1, max}$ -values and his growth rates are compared in Fig. 10. In both cases the growth rates are almost proportional to $Ra^{2/3}$. This means that they are inversely proportional to τ_c^* (see Eq. (10)). Since $r_0 = 1/(4\tau)$ from Eq. (9), the condition of $r_0 = r_1$ yields $r_1 = 1/(4\tau_c)$. Now, it is suggested that the condition of $r_0 = r_1$ is the measure to predict the onset of thermal instability, i.e., τ_c and a_c , for a given Ra and Pr .

CONCLUSION

In the present study the temporal evolution of disturbances in the fluid layer heated from below has been investigated theoretically for $Pr \rightarrow \infty$. Based on propagation theory, the Galerkin method has been employed. It is shown that the present Galerkin scheme is useful for $Ra \leq 10^4$. But it is believed that the results of $Ra = 10^4$ would be extended qualitatively to the case of a higher Ra . We here suggest a new measure to predict the onset of thermal instability and also that of manifest convection, based on the growth rates of the basic temperature field and its fluctuations. This new parameter ($r_1 = r_0$) will be very useful in pursuing more refined stability analysis for large- Pr systems.

ACKNOWLEDGMENTS

The authors acknowledge the support of LG Chemical Ltd., Seoul under the Brain Korea 21 Project of the Ministry of Education.

NOMENCLATURE

| | |
|--------------|--|
| a | : wavenumber |
| d | : depth of fluid layer |
| g | : gravitational acceleration |
| k | : heat conductivity |
| Nu | : Nusselt number, $q_w d / (k \Delta T)$ |
| Pr | : Prandtl number, ν / α |
| q_w | : bottom wall heat flux |
| r_0 | : growth rate of mean temperature |
| r_1 | : growth rate of temperature fluctuations |
| Ra | : Rayleigh number, $g \beta \Delta T d^3 / (\alpha \nu)$ |
| T | : temperature |
| \mathbf{u} | : velocity vector |
| w | : dimensionless vertical velocity, Wd / α |
| X | : spanwise coordinate |
| Z | : vertical coordinate |
| z | : dimensionless vertical coordinate, Z / d |

Greek Letters

| | |
|------------|--|
| α | : thermal diffusivity |
| β | : thermal expansivity |
| δ_r | : dimensionless thermal boundary-layer thickness |
| Δ_r | : dimensional thermal boundary-layer thickness |
| ν | : kinematic viscosity |
| θ | : dimensionless temperature, $T / \Delta T$ |
| τ | : dimensionless time, $t \alpha / d^2$ |
| ζ | : similarity variable, $z / \sqrt{\tau}$ |

Subscripts

rms : root-mean-square

i : initial condition

Superscript

' : perturbed state

REFERENCES

- Bénard, H., "Les Tourbillons Cellulaires Dan Une Nappe Liquide Transportant De La Chaleur Par Convection En Regime Permanent," *Ann. Chem. Phys.*, **23**, 62 (1901).
- Choi, C. K., Kang, K. H., Kim, M. C. and Hwang, I. G., "Convective Instabilities and Transport Properties in Horizontal Fluid Layers," *Korean J. Chem. Eng.*, **15**, 192 (1998).
- Elder, J. W., "The Temporal Development of a Model of High Rayleigh Number Convection," *J. Fluid Mech.*, **35**, 417 (1969).
- Foster, T. D., "Stability of a Homogeneous Fluid Cooled Uniformly from Above," *Phys. Fluids*, **8**, 1249 (1965).
- Foster, T. D., "Effect of Boundary Conditions on the Onset of Convection," *Phys. Fluids*, **11**, 1257 (1968).
- Gresho, P. M. and Sani, R. L., "The Stability of a Fluid Layer Subjected to a Step Change in Temperature: Transient vs. Frozen Time Analysis," *Int. J. Heat Mass Transfer*, **14**, 207 (1971).
- Herring, J. R., "Investigation of Problems in Thermal Convection," *J. Atmos. Sci.*, **20**, 325 (1963).
- Herring, J. R., "Investigation of Problems in Thermal Convection: Rigid Boundaries," *J. Atmos. Sci.*, **21**, 277 (1964).
- Hohenberg, P. C. and Swift, J. B., "Effects of Additive Noise at the Onset of Rayleigh-Benard Convection," *Phys. Rev. A*, **46**, 4773 (1992).
- Inoue, Y., Akutagawa, S., Saeki, S. and Ito, R., "Benard Convection of Electrolytic Solution in Electric Field," *Kagaku Kogaku Ronbunshu*, **9**, 359 (1983).
- Jhaveri, B. S. and Homay, G. M., "The Onset of Convection in Fluid Layer Heated Rapidly in a Time-dependent Manner," *J. Fluid Mech.*, **114**, 251 (1982).
- Kang, K. H., Choi, C. K. and Hwang, I. G., "Onset of Solutal Marangoni Convection in a Suddenly Desorbing Liquid Layer," *AIChE J.*, **46**, 15 (2000).
- Kim, M. C., Park, H. K. and Choi, C. K., "The Onset of Convective Instability of an Initially, Stably Stratified Fluid Subjected to a Step Change in Temperature," *Theoret. Comput. Fluid Dynamics*, **16**, 49 (2002).
- Koschmieder, E. L. and Pallas, S. G., "Heat Transfer Through a Shallow, Horizontal Convecting Fluid Layer," *Int. J. Heat Mass Transfer*, **17**, 991 (1974).
- Mahler, E. G., Schechter, R. S. and Wissler, E. H., "Stability of a Fluid Layer with Time-dependent Density Gradients," *Phys. Fluids*, **11**, 1901 (1968).
- Morton, B. R., "On the Equilibrium of a Stratified Layer of Fluid," *Quart. J. Mech. Appl. Math.*, **10**, 433 (1957).
- Patrick, M. A. and Wragg, A. A., "Optical and Electrochemical Studies of Transient Free Convection Mass Transfer at Horizontal Surfaces," *Int. J. Heat Mass Transfer*, **18**, 1397 (1975).
- Rayleigh, Lord, "On Convection Currents in a Horizontal Layer of Fluid when the High Temperature is on the Underside," *Phil. Mag.*, **32**, 529 (1916).
- Soberman, R. K., "Onset of Convection in Liquid Subjected to Transient Heating from Below," *Phys. Fluids*, **2**, 131 (1959).
- Yang, D. J. and Choi, C. K., "The Onset of Thermal Convection in a Horizontal Fluid Layer Heated from Below with Time-dependent Heat Flux," *Phys. Fluids*, **14**, 930 (2002).